Analysis of 3D Passive Walking Including Turning Motions for the Finite-width Rimless Wheel

A. Jaberi [1], M.R. Hairi Yazdi [2*] and M.R. Sabaapour [3]

1.Research Assistant in Control Laboratory, School of Mechanical Engineering, University of Tehran, Tehran, Iran

2. Associate Professor, School of Mechanical Engineering, University of Tehran, Tehran, Iran

3. PhD Candidate, School of Mechanical Engineering, University of Tehran, Tehran, Iran

Abstract

The focus of studies in the field of passive walking has often been on straight walking, while less attention has been paid to the field of turning motions. In this paper, the passive motions of a finite width rimless wheel as the simplest 3D model of passive biped walkers was investigated with a focus on turning motions. For this purpose, the hybrid model of the system consisting of continuous and discontinuous phases of motion was derived with respect to a vertical fixed frame that was independent of the surface profile. A Poincaré map corresponding to a step is one of the common methods used for the determination of periodic motions (limit cycles) and their specifications. In this study, it was emphasized that the Poincaré map has only one fixed point, indicating only one stable periodic motion that is parallel to the steepest slope surface. It is also shown that if the wheel is released from an orientation other than the steepest slope, the wheel turns towards the slope surface and eventually, its motion continues on the only existing stable limit cycle (passive limited turning). The effect of variation among some parameters of the initial conditions on rotational behaviour and its convergence were investigated.

1. Introduction

In recent decades, particular attention has been paid to the concept of passive walking in bipedal robots, due to the natural dynamic walking stability found in these types of walkers. Passive walking is a concept that was first defined and specifically investigated by McGeer [1], who showed that a passive walker can roll downward stably on an appropriately sloped surface only by its gravity force and without any actuators. Coleman also presented a comprehensive analysis of 3D passive walking [2], using a planar rimless wheel (zero width) model as a walker. A rimless wheel is a simple and appropriate model for walking analysis and has as its main features the motion of a passive biped robot. Coleman et al. indicated that a 2D

---

*Corresponding author, Tel: +98 21 88005677, Fax: +98 21 88013029, Email: myazdi@ut.ac.ir

rimless wheel on a sloped surface has a family of stable periodic motions that are equivalent to a set of stable limit cycles [3]. In addition, it was shown that the wheel had only one family of stable limit cycles. In further research, Smith et al. used a finite width rimless wheel [4]. Having hip width and leg separation, their proposed model can be more useful for understanding 3D bipedal locomotion. However, their analysis had been based on a fixed frame coordinate normal to the slope surface, which is not adequate for applying to turning analysis in the current paper.

In this paper, we deal with the turning motion of the finite width rimless wheel. We present a new comprehensive model with respect to a general vertical fixed frame coordinate that is independent of the surface profile. Humans often use turning motions in their daily activities to improve their performance when walking and for obstacle avoidance. Recently, Sabaapour et al. investigated the limited and continuous turning of a 2D rimless wheel on a sloped surface [5, 6]. In this paper, the results of the above work have been implemented for the finite width rimless wheel in order to exploit the advantages of this model.

In addition to the development of the passive walking concept, some of its features such as natural stability and high energy efficiency have also been utilized in the design of a more effective active controller for walking on a flat surface [7, 8]. Similarly, the results of this paper can be applied to the design of a more effective steering controller for biped robots. However, this issue is beyond the scope of the present research.

This paper is organized as follows: the 3D passive motion of the hybrid model of a system on a sloped surface, including the description of the continuous and discontinuous phases and their equations, are investigated in the first section. In the next section, the stability of periodic motion and its corresponding limit cycles are analysed. In this section, the effect of variation on some parameters pertaining to the stability of the limit cycle and its convergence are also investigated. Finally, a conclusion and future research are presented.

2. Description of the system

In this section, the general dynamic equations of motion of the finite width rimless wheel on a gentle slope are presented. Referring to Figure 1, the physical parameters of the system are as follows: the total mass of the wheel is m and each leg of the wheel has length R. Additionally, the width of the wheel is w and the angle between each two consecutive spokes located on two opposite planes is $2\alpha_w = 2\pi / n$, while n is the number of spokes of the wheel that rolls down a gentle slope of angle γ. In addition, the principle moments of inertia about the axes of body fixed coordinate frame i.e., x, y and z are I_0, $2I_0$ and I_0, respectively, where it is assumed that $I_0 = 1/4\, mR^2$.
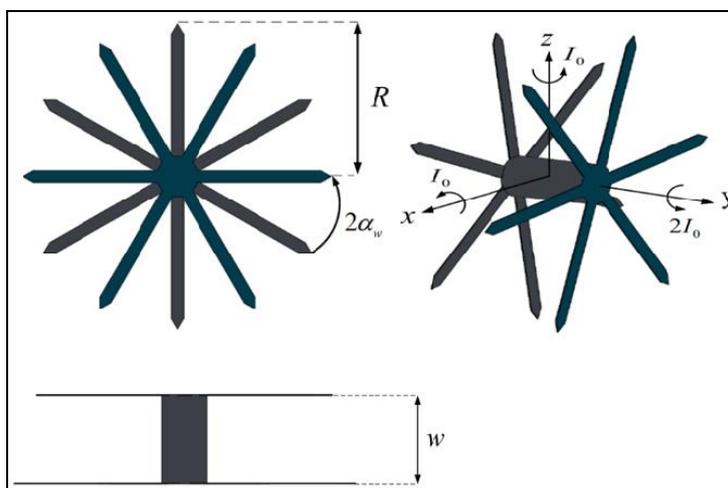
Fig. 1. Schematic of the finite width rimless wheel

2.1. Single support or continuous phase

In this phase, the wheel rotates about the contact point as an inverse pendulum between two consequent collisions. The general equations of motion driven using the Lagrange method are:

$$M(q)\ddot{q} + C(q,\dot{q})\dot{q} + G(q) = 0 \qquad (1)$$

where q is the generalized coordinate of the system. The state space form of Equation (1) leads to:

$$\dot{\mathbf{x}} = \begin{bmatrix} \dot{q} \\ M^{-1}(q)\left[-C(q,\dot{q}) - G(q) \right] \end{bmatrix} =: f(x) \qquad (2)$$

where $x = \begin{bmatrix} q & \dot{q} \end{bmatrix}^T$. It is assumed that the wheel rolls around the support leg without slipping or the loss of contact until the next collision. It can be assumed that the contact point behaves as a spherical joint in this phase. Therefore, the wheel has three rotational degrees of freedom about the contact point. As can be seen in Figure 2, the state variables of the wheel are defined as:

$$q = \begin{bmatrix} \phi & \psi & \theta \end{bmatrix}^T \qquad (3)$$

where ϕ, ψ and θ are the heading, lean and pitch angles, respectively, defined in the body coordinate frame.
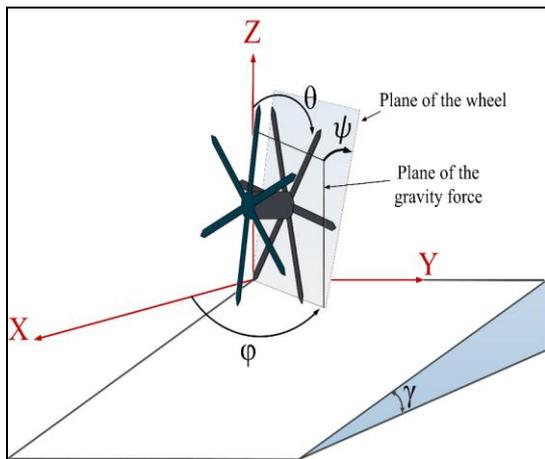
Fig. 2. Three DOF of the finite rimless wheel on a slope (from [5], with minor differences)

In this instance, a 3-1-2 (ZXY) Euler angles convention is used to represent the orientations of the wheel in each instant of the motion. The velocities and accelerations in Eq. (2) are assumed to have been normalized with respect to the non-dimensional time. Additionally, other parameters such as length, mass and moment of inertia have been normalized with respect to m and R.

2.2. Double support or transition phase

This phase begins immediately prior to collision up to immediately following collision. To avoid complexity, collisions are assumed to be rigid and perfectly plastic. Thus, the amounts of heading and lean angles immediately before and after collision do not change. It should be noted that the pitch angle must be reset at the start of each step. Angular momentum conservation around the contact point is used to obtain the angular velocities after collision. Notably, the angular momentum variations caused by the force of weight are ignored. Accordingly, we have:

$$H_c^+ = H_c^- \qquad (4)$$

where

$$H_c^- = \bar{I}\omega^- + r_{G/c} \times mv_G^- \qquad (5)$$

$$H_c^+ = \bar{I}\omega^+ + r_{G/c} \times mv_G^+ \qquad (6)$$

The superscripts "-" and "+" indicate the instantaneous before and after collisions, respectively. Finally, the angular velocities after each collision will be related as follows:

$$\begin{bmatrix} \dot{\phi}^+ \\ \dot{\psi}^+ \\ \dot{\theta}^+ \end{bmatrix} = M \begin{bmatrix} \dot{\phi}^- \\ \dot{\psi}^- \\ \dot{\theta}^- \end{bmatrix} \qquad (7)$$

where M is the mapping matrix at the impact phase. We must have a collision detection function with which to compute M. The collision condition in the vertical fixed coordinate system is:

$$z_r = x_r \tan(\gamma) \qquad (8)$$

where x_r and z_r are the x and z components of the swing leg in the collision position. Unlike a planar rimless wheel, Euler angles are dependent in a double support phase [5] that is obtained from Equation (8):

$$\cos\psi(\sin\theta - \cos\theta\tan\alpha_s) + w/2R\sin\alpha_s\cos\alpha_s\ (\sin\psi + \cos\psi\sin\varphi\tan\gamma)$$
$$+ \tan\gamma\left[(\sin\theta\cos\varphi + \cos\theta\sin\psi\sin\varphi)\tan\alpha_s + (\cos\theta\cos\varphi - \sin\theta\sin\psi\sin\varphi)\right] = 0 \tag{9}$$

3. Stable Limited Turning

One of the methods for finding the periodic motions and conducting the stability analysis for such hybrid systems is Poincare sections [9], which are identified by:

$$^{k+1}\mathbf{x}^+ = \mathrm{P}(^k\mathbf{x}^+) \tag{10}$$

where *P(0)* is the Poincare map that maps the states of the system after only one collision, $^k\mathbf{x}^+$, to only after the next one, $^{k+1}\mathbf{x}^+$. To have periodic motion, the wheel must roll down with these particular initial conditions. In other words, there are particular initial conditions that the states of the system return to their conditions that they started from via Poincare map, i.e.:

$$\mathbf{x}^* = \mathrm{P}(\mathbf{x}^*) \rightarrow \mathbf{x}^* - \mathrm{P}(\mathbf{x}^*) = 0 \tag{11}$$

These states are called *fixed points* and their periodic motion follows a *limit cycle*.

In the case of the 3D finite-width rimless wheel, when it lies on a stable limit cycle, the states return to their values after two consecutive steps (a gait cycle). Coleman et al. investigated the 3D motion analysis of a planar rimless wheel and showed that with different fixed points, the wheel had a family of periodic motions or limit cycles that were locally asymptotically stable [3].

In the current paper, unlike the planar rimless wheel, it is shown that as long as the physical parameters of the finite width rimless wheel and the slope surface remain unchanged, the wheel has only a unique fixed point that is, parallel to the steepest descent. In other words, the Poincare map has only one fixed point, which can be obtained via a numerical optimization method such as the Newton-Raphson method. Thus, Equation (11) is solved numerically in order to find this fixed point. For this simulation, *a*= 2π/16 (*rad*), *w=0.1R* and γ=0.1(*rad*) have been considered. The fixed point here is obtained as:

$$\mathbf{x}^* = \{\phi^* = 0.0002768, \psi^* = -0.0016, \theta^* = -0.09684$$
$$, \dot\phi^* = 0.0, \dot\psi^* = 0.0, \dot\theta^* = 0.6849\}^T \tag{12}$$

Then, an arbitrary initial condition is represented by:

$$\mathbf{x}_0 = \{0.56, 0.01, -0.1095, 0, 0, 0.7496\} \tag{13}$$

The state variations of more than 350 steps are illustrated in Figure 3.

In Figure 3, although the wheel is released from a non-equilibrium initial condition, it turns enough to lie on the stable limit cycle. Therefore, this locomotion can be considered as a limited turning motion. Roughly speaking, the fixed point indicates a periodic gait that is parallel to the steepest descent of the slope surface, i.e., the heading angle becomes zero in the steady gait.
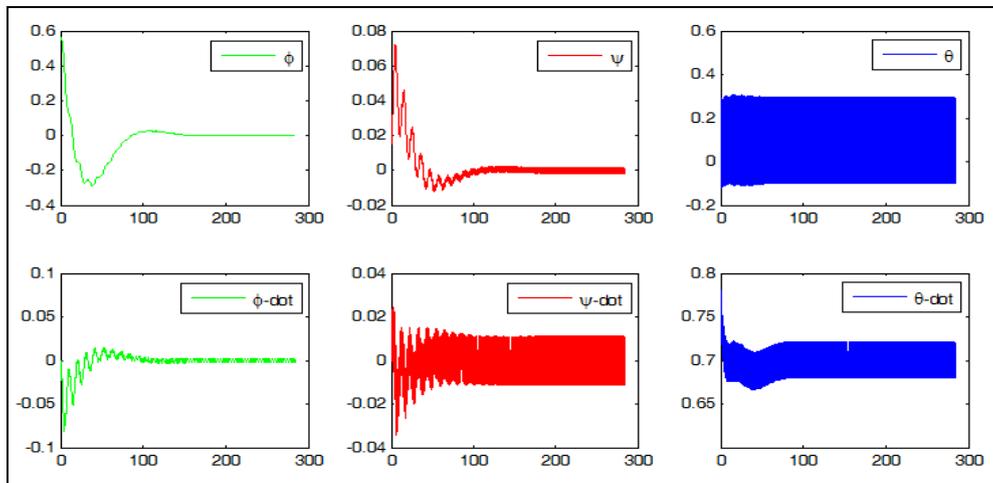
Fig. 3. State variables of more than 350 steps representing passive limited turning on a gentle slope. Note that the horizontal axis is non-dimensional time in all sub-figures (vertical axes are also non-dimensionalized).

Furthermore, the wheel is modelled in ADAMS for validating the MATLAB results. The state variables are compared for 50 steps, released from an arbitrary initial condition (Figure 4). As is shown, the results are matched and show little difference. The differences are the result of the authors having been unable to exactly simulate an ideal and perfectly plastic collision in ADAMS. It should be noted that in the case of pitch angle (θ), the amount of steps had been accumulated in ADAMS.
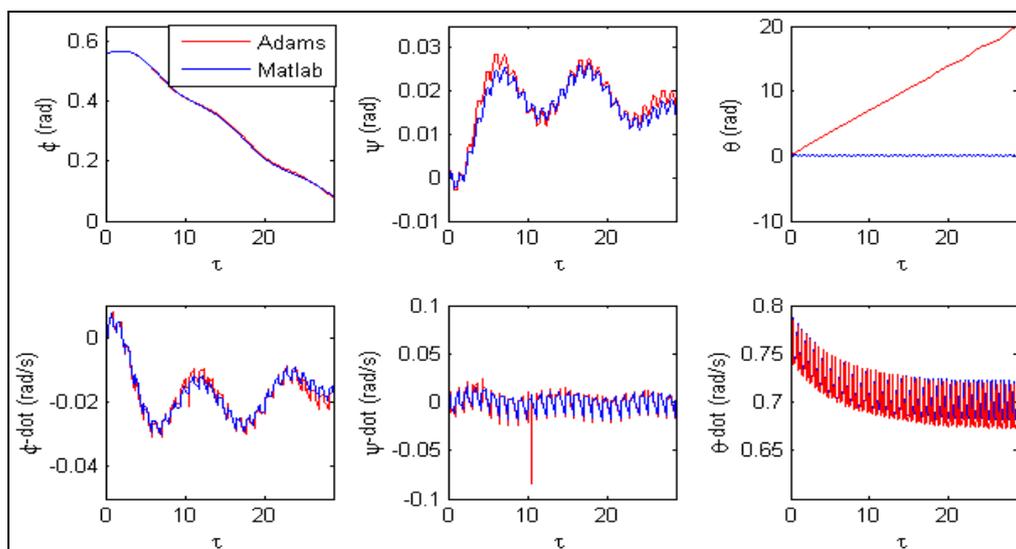
Fig. 4. Comparison the MATLAB and ADAMS results for 50 steps from an arbitrary initial condition shown as

$$X_0 = \begin{bmatrix} 0.56, 0.001, 0, 0, 0, 0.7496 \end{bmatrix}^T$$

In order to compare these results, different initial heading and lean angles were assumed and the simulated system is shown in Figure 5 and Figure 6 As is shown, as the initial heading and lean angles increased, the wheel was expected to have to turn more frequently in order to maintain stability. Notably, the wheel was locally asymptotically stable with a limited basin of attraction. Therefore, it fell down for $\psi_0 > 0.05$ (rad) and $\phi_0 > 1.08$ (rad), as depicted in Figure 5 and 6, respectively.
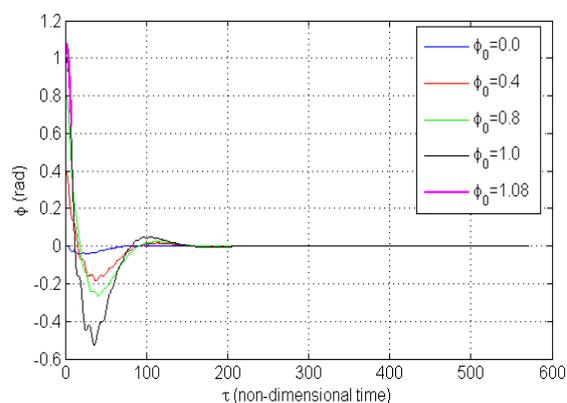
Fig. 6. Effect of different initial heading angle (ϕ_0) on a passive limited turning (heading angle)

Furthermore, in order to have a better understanding of bipedal passive turning locomotion, the 3D contact position of the stance leg with the ground was illustrated for different initial headings and lean angles in Figures 7 and 8, respectively. As expected, all paths eventually became parallel to the steepest descent of the sloped surface in the final steady gait.

Fig. 5. Effect of different ψ_0 on a passive limited turning (heading angle)
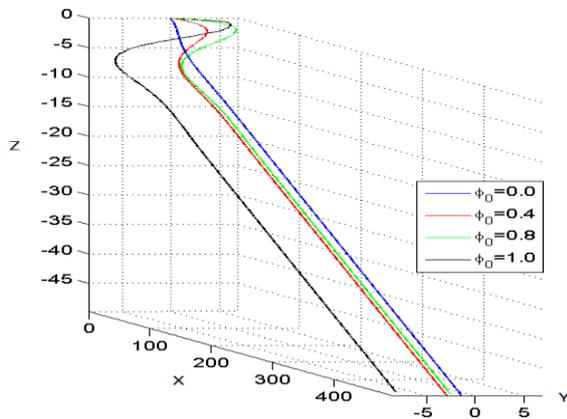
Fig. 7. Foot position (3D) of the wheel for a different initial heading angle. All dimensions are given in m.
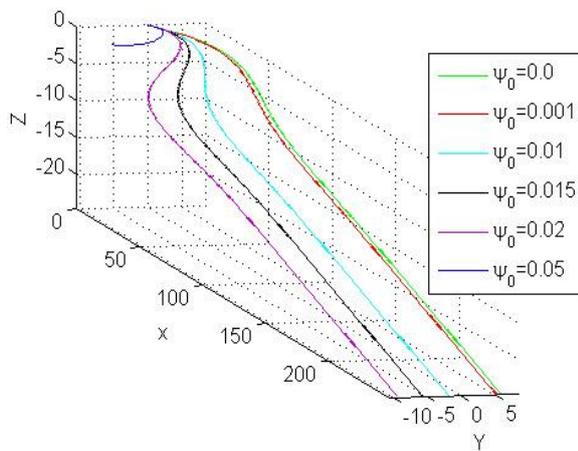
Fig. 8. Foot position (3D) of the wheel for a different initial lean angle (ψ_0). All dimensions are given in m.

4. Conclusion

In this study, we investigated the passive limited turning of a finite width rimless wheel on a sloped surface. A new comprehensive hybrid model of the wheel, independent from the ground surface profile, was presented. Then, a Poincare section was used for the determination of periodic motions (limit cycles). It was shown that the Poincare map had only one fixed point representing a periodic motion. The primary feature of this limit cyclic gait was that it was parallel to the steepest descent of the ground. Moreover, we have shown that by changing some parameters, the wheel reverted to its limit cycle. Future research in this area might include discovering asymptotically stable passive continuous turning.

References

[1]. McGeer, T., 1990, Passive dynamic walking, *The International Journal of Robotics Reseach,* **9**(2), pp. 62-82.

[2]. Coleman, M.J. 1998, A stability study of a three-dimensional passive dynamic model of human gait, Cornell University, PhD thesis.

[3]. Coleman, M.J., Chatterjee, A. and Ruina, A., 1997, Motions of a rimless spoked wheel: a simple three-dimensional system with impacts, *Dynamics and Stability of Systems,* **12**(3), pp. 139-159.

[4]. Smith, A. C. and Berkemeier, M. D., 1998, The motion of a finite-width rimless wheel in 3D, in *Robotics and Automation Proceedings IEEE International Conference*, Leuven, Belgium.

[5]. Sabaapour, M.R., Hairi-Yazdi, M.R. and Beigzadeh, B., 2014, Towards passive turning in biped walkers, *Procedia Technology,* **12**, pp. 98-104.

[6]. Sabaapour, M. R., Hairi-Yazdi, M. R., and Beigzadeh, B., 2014, Passive turning motion of 3D rimless wheel: novel periodic gaits for bipedal curved walking, *Submitted to Advanced Robotics.*

[7]. Spong, M. W., and Bullo, F., 2002, Controlled symmetries and passive walking, in *in Proc. 15th Triennial World Congress..*

[8]. Goswami, A., Espiau, B., and Keramane, A., 1997, Limit cycles in a passive compass gait biped and passivity-mimicking control laws, *Autonomous Robots,* **4**(3), pp. 273-286.

[9]. Shih, C., Grizzle, J.W. and Chevallereau, C., 2009, Asymptotically stable walking and steering of a 3D bipedal robot with passive point feet, *IEEE Transactions on Robotics.*